EUROPEAN ORGANIZATION FOR NUCLEAR RESEARCH
CERN – ACCELERATORS AND TECHNOLOGY SECTOR

Thoughts about Gantries

Eberhard Keil

Abstract

The section 2007 FFAG gantry reviews an FFAG gantry, which transport beams with momenta varying by about a factor of two at constant excitation, well matched to FFAG accelerators. The section FODO gantry describes pulsed gantries with magnet excitation proportional to the beam momentum, and a small difference between beam and design momentum. They are well matched to pulsed synchrotrons. The dispersion in the bending plane need not be controlled as tightly as in the FFAG gantries. Nearly round beams are obtained in the tumor at the rotation axis by operating with much smaller phase advances in the plane perpendicular to the median plane. Scanning, installed between the end of the gantry lattice and the rotation axis, is briefly discussed in the section Scanning.

INTRODUCTION

Together with coauthors, I published on medical accelerators and gantries between 2004 and 2007 in journals [1, 2], conferences [3, 4, 5, 6, 7], and workshops [8, 9, 10]. Most papers can also be found at http://keil.home.cern.ch/keil/pub.html . Trbojevic continued work on gantries [11, 12]. The next section, entitled 2007 FFAG gantry, reviews an example of FFAG gantries published in 2007 [2], which transport beams with momenta varying by about a factor of two at constant excitation. The section, entitled FODO gantry, describes pulsed gantries, where the magnet excitation is proportional to the beam momentum, and the difference between beam and design momentum is small. Hence the dispersion in the bending plane D_x need not be controlled as tightly as in the FFAG gantries. I discuss the design of such FODO gantries in several stages. For no particular reason, I do calculations and plot graphs sometimes up to the end of the gantry lattice and sometimes up to the rotation axis of the gantry. The gantry lattice ends a few metres from the rotation axis, where the tumour is located. The gantries in this report have a family resemblance. The arcs consist of periodic cells that are repeated a number of times. The β-functions in the arcs are at least very close to their periodic values in the cells. In the 2007 FFAG gantry, also the dispersion in the plane of the gantry in the arcs is at least very close to its periodic value in the cells. In the FODO gantries I use forced oscillations of the dispersion in the plane of the gantry to achieve my goals. This approach to gantry design is quite different to the design of existing gantries that consist essentially of individual magnets with individual excitations, adapted to their purpose [13, 14]. The planned PAMELA gantry [15] is quite similar to our FFAG gantry.

In the section entitled scanning, I discuss my assumptions about the beam optics and scanning between the end of the gantry lattice and the rotation axis . The last section gives my conclusions.
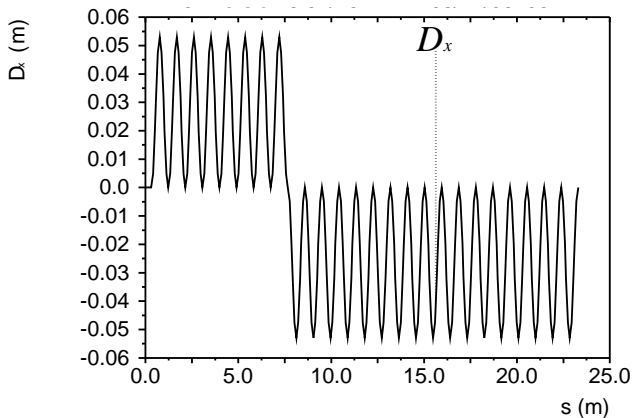

Figure 1: Horizontal dispersion D_x in the FFAG gantry [2] up to the end of the FFAG lattice

2007 FFAG GANTRY

Our FFAG gantries were designed such that they transported beams over a range of about a factor of two in momentum at fixed excitation. This would allow changes in the beam momentum from pulse to pulse, as foreseen in our non-scaling FFAG rings [7] accelerating in about 1.7 ms at most. Our FFAG gantries were designed like our non-scaling FFAG accelerators with periodic cells, not like beam lines with magnets of individual shapes and individual excitations. We assumed that the beam emittances in the two transverse planes are equal. This assumption may not be justified, in particular in slowly ejected beams from synchrotrons [16]. We made the beam round at the point in the beam line from the accelerator where the rotation of the gantry starts by having equal β-functions and $\alpha = 0$ in the two planes. We assumed that the dispersion D and its derivative D' vanish at this point. A telescope matched the equal β-functions to the periodic values in the gantry cells. An example of a very short telescope, matched with MAD Version 8, is mentioned in [2]. It consisted of two quadrupoles and two drift spaces. Its length was about 0.3 m. All gantries, the FFAG gantries in this section and the FODO gantries in the next section, have in common that the sign of the curvature changes, i.e. an upwards (left) bend is followed by a downwards (right) bend. It is convenient for the matching, if $D = D' = 0$ at the point where the curvature changes sign, and also at the exit of the gantry. In [2] we achieved these goals by symmetrical triplet cells that have $D = D' = 0$ at one point along every cell. Fig. 1 is reproduced from [2], and shows the dispersion D_x. The β-functions are simply periodic with the cells, not affected by the change of the sign of the curvature, and similar to those shown in Fig. 4.
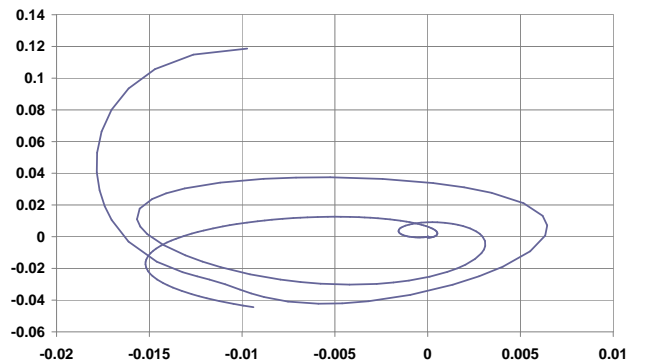

Figure 2: Horizontal slope x' in rad at the end of the 2007 FFAG gantry lattice dec17g vs. horizontal position x in m. The parameter is the momentum error $-0.3 \leq \delta p/p \leq +0.3$.

This approach has the advantage that the number of cells in the upwards and downwards arcs may be any positive integer. Because of the FFAG principle with reverse bends in every cell, the maximum value of D_x is also pretty small at $|D_x| < 60$ mm. At momenta different from the design momentum, the beam offsets x and slopes x' in the plane

Table 1: FODO gantries: Parameters cell length, horizontal and vertical cell tunes, β-functions on rotation axis after drift of length d from end of gantry, maximum distance of gantry orbit from rotation axis R, dipole field B and gradients G_F and G_D of focusing and defocusing combined-function magnets

File	aug15h	nov16h	nov16i	nov16j	nov16k	nov16l	nov16m
Cell length/m	1.58	1.38	2.58	2.58	1.98	1.38	1.38
Hor. cell tune	1/4	1/3	1/3	1/4	1/5	1/3	1/3
Vert. cell tume	1/4	1/3	1/3	1/4	1/5	1/6	1/6
β_x/m	7.53	6.75	7.08	8.89	7.14	7.27	7.45
β_y/m	25.09	42.99	25.2	23.99	14.18	14.81	9.33
R/m	5.67	4.98	7.50	8.78	7.72	4.98	4.98
d/m	3.329	3.229	3.329	4.399	3.521	3.229	3.229
B/T	3.114	4.149	2.074	1.557	1.661	4.149	4.149
G_F/Tm^{-1}	35.76	44.18	12.08	9.80	13.97	41.49	40.72
G_D/Tm^{-1}	-35.12	-42.95	-11.87	-9.69	-13.84	-31.77	-28.91

of bending at the end of the gantry do not vanish. Fig. 8 in [1] shows them clearly. Fig. 2 shows another view of the horizontal slope x' vs. the horizontal position x at the end of the FFAG gantry lattice. The small loop near the origin occurs at $\delta p/p \approx 0$. The position x is inside a range -15 mm $\leq x \leq +5$ mm as expected. The slope remains inside the approximate range $|x'| \leq 40$ mr for $-0.29 \leq \delta p/p \leq +0.3$.
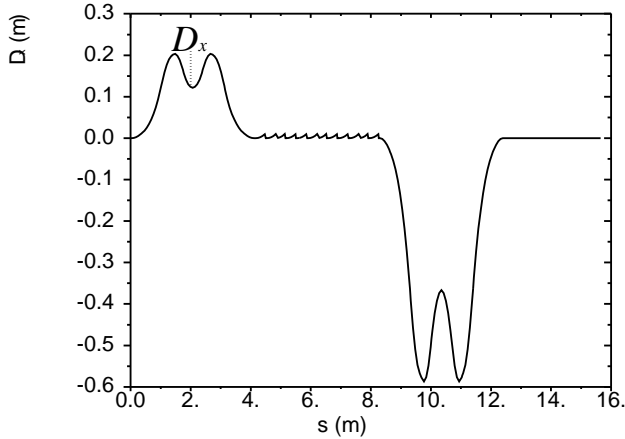

Figure 3: Horizontal dispersion D_x in the FODO gantry nov16m up to the rotation axis; the wiggles at $4 < s < 8$ m are caused by the interpolation.

FODO GANTRIES

If the accelerator, e.g. a cyclotron, delivers beam at one fixed energy or if the accelerator, e.g. a synchrotron, is pulsed, the gantry can be excited or pulsed such that the beam momentum is close to the design momentum, and extremely small values of D are not needed. Such gantries need not be designed as FFAG gantries with reverse bends, but can be designed as FODO gantries with equal dipole fields in F and D magnets. At the same average radius R, the dipole fields are much smaller than in FFAG gantries. I

still want $D = D' = 0$ at start and end of the gantry and at the point where the curvature changes sign. There is no FODO cell with $D = D' = 0$ in one point, hence I am obliged to work with forced oscillations of D. I put exactly one betatron wavelength into the upwards and downwards bends, respectively, by satisfying the condition $Nq = 1$ on the cell tune in the bending plane q and the number of cells N. I can adjust the distance from the end of the gantry to the rotation axis by inserting straight cells between the upwards and downwards arcs. Fig. 3 shows the manipulations of the dispersion D_x. D_x vanishes in the straight cells between the arcs and between the end of the gantry and the rotation axis. D_x is three times larger in the downwards than in the upwards arc, since the bending angles in a cell are three times larger there.
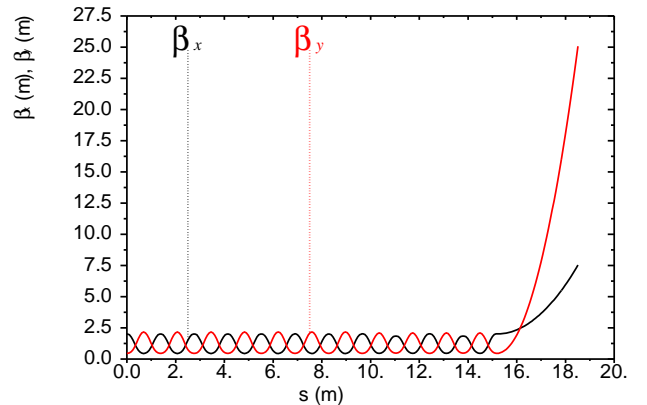

Figure 4: Orbit functions β_x and β_y in the FODO gantry aug15h up to the rotation axis

Tab. 1 shows the first batch of my results. In [17] are input and output files of the FODO gantry aug15h. The maximum distance R of the orbit from the rotation axis is about 5.67 m, and the distance between the end of the gantry and the rotation axis is about 3.33 m. The cell tunes in both transverse planes are 0.25. Since combined function dipoles have edge focusing, I must match the gradi-

ents of the upwards and downwards arcs and of the straight cells to the desired cell tunes separately. The values of β_x and β_y at the boundaries of the CELL, RCELL and SCELL periods are still slightly different, and there remains a mismatch in the whole gantry.

The authors of [18] assume $\beta = 1$ m in both planes in their simulation of the scanning system. Their paper prompted me to write to them, saying that their gantry was over-focused. I meant that the β-functions at the end of the gantry were too small for an efficient transport through a drift space of a few metres. The minimum value of β at the end of a drift space of length d is achieved when $\beta = d$ and the initial $\alpha = 0$. Fig. 4 shows the orbit functions β_x and β_y in the FODO gantry aug15h. At the end of the gantry proper, the β-functions are about 2 m in the plane of the bending and 0.45 m in the plane perpendicular to it. In the latter plane, the β-function at the rotation axis is particularly large at $\beta \approx 25$ m. One way of increasing the betatron wavelength is increasing the cell length at constant cell tune. A way of increasing the β-function out of the bending plane is reducing the cell tune in that plane. Note that there is no condition on the cell tune as there is in the bending plane. The gantries no16h.txt, nov16l.txt and nov16m.txt in Tab. 1 have the same shape. By the time I reached the nov16m gantry in the rightmost column of Tab. 1, I knew that I can achieve $\beta_x \approx \beta_y$ on the rotation axis by having a vertical cell tune that is much smaller than the horizontal one (in the bending plane).

I continued exploring and matching gantries with smaller vertical cell tunes, summarized in Tab. 2. Data and some results are in [19]. In the nov16t gantry in the rightmost column, the minimum of β_y is equal to the maximum of β_x in the cells of the upwards arcs. Only the unavoidable slight mismatch along the gantry prevents them from being equal also at the rotation axis, as can be seen in Fig. 5, where $\beta_x = \beta_y$ at $s = 0$. Hence, the telescope mentioned in the Section about FFAG gantries is not needed.
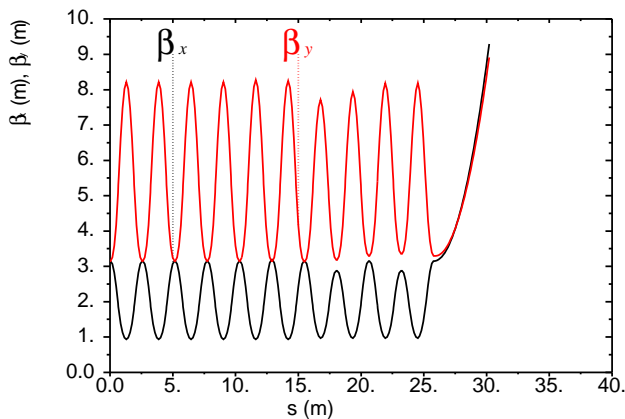

Figure 5: β_x and β_y in the FODO gantry nov16t

Fields and gradients are shown in Tabs. 1 and 2 for C^{6+} ions with 400 MeV/u kinetic energy, and a magnetic rigidity $B\rho = 6.345$ Tm. The gantries come in two classes, those with dipoles fields B smaller than about 2 T, which can be built with resistive room-temperature magnets, and those with higher fields, which must use super-conducting magnets.

SCANNING

I assume that there is a drift space between the end of the gantry lattice and the rotation axis. Trbojevic and collaborators [11, 12] use an essentially focus-to-parallel optical system there. I have not looked at such optical systems. In either case, the orbit functions at the end of the gantry lattice and at the rotation axis are related, and the desired orbit functions at the rotation axis determine those at the end of the gantry lattice. The FFAG and FODO gantry lattices discussed here have in common that their apertures are rather small. Hence, the weights of the magnets and of the whole gantry are also rather small. Because of the small aperture, the scanning equipment must be installed between the end of the gantry lattice and the rotation axis. It moves the beam by about ±0.1 m in both directions perpendicular to the beam axis. There are two alternatives for the scanning system. One can either use two magnets that deflect the beam in two perpendicular directions, such that they fan out between the scanning magnets and the rotation axis. Such a system has the advantages, that the deflection angles are of order ±0.1 m/4 m = 25 mrad, and that the apertures of the scanning magnets are not much larger than those in the gantry lattice, and the disadvantage that the skin dose is higher than in the second system by about $[4 \text{ m}/(4 \text{ m} - 0.2 \text{ m})]^2 - 1 \approx 11\%$ [16]. In this second system, two magnets are used in each direction, the second magnet cancelling the deflection of the first one. Hence, the beams approaching the rotation axis are all parallel. Such a system has the advantages that the skin dose in not enhanced by the fanning out, and that the planning of the treatment may be easier, but it also has disadvantages. In the scanning system studied in [18], the deflection angles are about 125 mrad, and the aperture of the last magnet must be of order $0.2 \text{ m} \times 0.2$ m. If x and x' at the end of the gantry were small enough that they are minor perturbations compared to the offsets and slopes during scanning, they could be handled by the software that drives the scanning magnets. Fig. 2 shows that this is not true in the first, but marginally true in the second scanning system above.

CONCLUSIONS

After an introduction, giving most of the references, the FFAG gantry, published in 2007, is reviewed. It transports H^+ or C^{6+} beams with momenta varying by about a factor of two at constant field, and is well matched to FFAG accelerators. Then, pulsed "FODO" gantries are presented. They are well matched to pulsed synchrotrons. The desired behaviour of the dispersion is achieved by forced oscillations. Nearly round beams are obtained in the tumor at the rotation axis by operating with much smaller phases

Table 2: More FODO gantries: Parameters cell length, horizontal and vertical cell tunes, β-functions on rotation axis after drift of length d from end of gantry, maximum distance of gantry orbit from rotation axis R, dipole field B and gradients G_F and G_D of focusing and defocusing combined-function magnets

File	nov16n	nov16o	nov16p	nov16q	nov16r	nov16s	nov16t
Cell length/m	2.58	2.58	2.58	2.58	2.58	2.58	2.58
Hor. cell tune	1/3	1/4	1/4	0.2514	1/4	0.2500	0.2500
Vert. cell tume	1/10	1/8	1/10	0.0887	0.085	0.0851	0.0851
β_x/m	7.01	9.26	9.26	9.28	9.29	9.29	9.29
β_y/m	7.26	11.47	9.58	9.48	8.91	8.91	8.91
R/m	5.75	8.78	8.78	8.78	8.78	8.78	8.78
d/m	3.227	4.399	4.399	4.399	4.399	4.399	4.399
B/T	2.766	1.557	1.557	1.557	1.557	1.557	1.557
G_F/Tm^{-1}	18.46	8.81	8.65	8.59	8.56	8.56	8.56
G_D/Tm^{-1}	-11.65	-7.14	-11.87	-6.76	-6.60	-6.57	-6.57

advances in the plane perpendicular to the median plane. Scanning is briefly discussed in the next section. According to our design principles, it must be installed between the end of the gantry lattice and the rotation axis.

REFERENCES

[1] D. Trbojevic, B. Parker, E. Keil, A.M. Sessler, Carbon/proton therapy: A novel gantry design, PRSTAB **10** (2007) 053503.

[2] E. Keil, A.M. Sessler, D. Trbojevic, Handron cancer therapy cemplex using onscaling fixed field alternating gradient and gantry design, PRSTAB **10** (2007) 054701.

[3] D. Trbojevic, A.G. Ruggiero, E. Keil, N. Neskovic, A.M. Sessler, Design of a Non-Scaling FFAG Accelerator for Proton Therapy, http://accelconf.web.cern.ch/AccelConf/c04/data/CYC2004_papers/19P31.pdf (2004).

[4] E. Keil, D. Trbojevic,A.M. Sessler, Fixed Field Aletrnating Gradient Accelerators (FFAG) for Hadron Cancer Therapy, PAC (2005) 1667.

[5] E. Keil, A.M. Sessler, D. Trbojevic, Hadron Cancer Therapy Complex Employing Non-Scaling FFAG Accelerator and Fixed Field Gantry Design, EPAC (2006) 1681.

[6] D. Trbojevic, R. Gupta, B. Parker, E. Keil and A.M. Sessler, A Dramatically Reduced Size in the Gantry design for the Proton-Carbon Therapy, EPAC (2006) 2352.

[7] E. Keil, A.M. Sessler, D. Trbojevic, Three-Ring FFAG Complex for H$^+$ and C^{6+} Therapy, Cyclotrons (2007) 193.

[8] E. Keil, A.M. Sessler, D. Trbojevic, A Non-Scaling Radial-Sector Fixed Field Aletrnating Gradient (FFAG) Ring for Carbon Cancer Therapy, http://keil.home.cern.ch/keil/Doc/Conferences/04OctFFAG/proceed.pdf (2004)

[9] E. Keil, A.M. Sessler, D. Trbojevic, Hadron Cancer Therapy Complex Employing Non-Scaling FFAG Accelerator and Fixed Field Gantry Design, http://hadron.kek.jp/FFAG/FFAG06_HP/proceeding/07keil.pdf (2007)

[10] E. Keil, A.M. Sessler, D. Trbojevic, Recent Developments in Our Hadron Cancer Therapy Complex, http://indico.in2p3.fr/conferenceDisplay.py?confId=115 (2007).

[11] D. Trbojevic, Update on the Innovative Carbon/Proton Non-Scaling FFAG Isocentric Gantries for Cancer Therapy, IPAC10 (2010) 124.

[12] D. Trbojevic and V. Morozov, Innovative Superconducting Non-Scaling Fixed Field Alternating Gradient Isocentric Gantry fro Carbon Cancer Therapy, IPAC2011 (2011) 2544.

[13] M. Galonska et al., Commissioning of the Ion Beam Gantry at HIT, IPAC2011 (2011) 2874.

[14] E. Pedroni et al., Pencil beam characteristics of the next-generation proton scanning gantry of PSI: design issues and initial commissioning results, Eur. Phys. J. Plus (2011) 126:66.

[15] R. Fenning et al., A Non-Scaling Gantry Design for the PAMELA Project, IPAC (2010) 4593.

[16] D. Brandt CERN, private communication (2011).

[17] http://keil.home.cern.ch/keil/MadX/2011/Aug2011/15Aug11/

[18] C. Sun et al., Compact Beam Delivery Systems for Ion Beam Therapy, IPAC (2011) 3633.

[19] http://keil.home.cern.ch/keil/MadX/2011/Nov2011/16Nov11/